Hierarchical Fuzzy Systems Integrated with Particle Swarm Optimization for Daily Reference Evapotranspiration Prediction: A Novel Approach

Dilip Kumar Roy (dilip.roy@my.jcu.edu.au)
Bangladesh Agricultural Research Institute https://orcid.org/0000-0002-7685-0445
Kowshik Kumar Saha
Technical University of Berlin: Technische Universitat Berlin
Mohammad Kamruzzaman
Bangladesh Rice Research Institute
Sujit Kumar Biswas
Bangladesh Agricultural Research Institute
Mohammad Anower Hossain
Bangladesh Agricultural Research Institute

Research Article

Keywords: Reference evapotranspiration, Hierarchical fuzzy systems, Fuzzy inference system, Regression tree, M5 model tree, Shannon's entropy

Posted Date: July 21st, 2021

DOI: https://doi.org/10.21203/rs.3.rs-617105/v1

Version of Record: A version of this preprint was published at Water Resources Management on November 3rd, 2021. See the published version at https://doi.org/10.1007/s11269-021-03009-9.

Hierarchical fuzzy systems integrated with particle swarm optimization for daily reference evapotranspiration prediction: A novel approach

Dilip Kumar Roy[a*], Kowshik Kumar Saha[b], Mohammad Kamruzzaman[c], Sujit Kumar Biswas[a] and Mohammad Anower Hossain[a]

[a]Irrigation and Water Management Division, Bangladesh Agricultural Research Institute, Gazipur – 1701, Bangladesh
[b]Department of Agromechatronics, Technical University of Berlin, 10623 Berlin, Germany
[c]Farm Machinery and Postharvest Technology Division, Bangladesh Rice Research Institute, Gazipur-1701, Bangladesh

*Corresponding author email: dilip.roy@my.jcu.edu.au

Abstract

Reference evapotranspiration (ET_0) is a crucial element for deriving a meaningful scheduling of irrigation for major crops. Thus, precise projection of future ET_0 is essential for better management of scarce water resources in many parts of the globe. This study evaluates the potential of a Hierarchical Fuzzy System (HFS) optimized by Particle Swarm Optimization (PSO) algorithm (PSO-HFS) to predict daily ET_0. The meteorological variables and estimated ET_0 were employed as inputs and outputs, respectively, for the PSO-HFS model. The FAO 56 PM method to ET_0 computation was implemented to obtain ET_0 values using the climatic variables obtained from two weather stations located in Gazipur Sadar and Ishurdi, Bangladesh. Prediction accuracy of PSO-HFS was compared with that of a FIS, M5 Model Tree, and a Regression Tree (RT) model. Several statistical performance evaluation indices were used to evaluate the performances of the PSO-HFS, FIS, M5 Model Tree, and RT in estimating daily ET_0. Ranking of the models was performed using the concept of Shannon's Entropy that accounts for a set of performance evaluation indices. Results revealed that the PSO-HFS model performed better than the tree-based models.

Generalization capabilities of the preposed models were evaluated using the dataset from a test station (Ishurdi station). Results revealed that the models performed equally well with the unseen test dataset, and that the PSO-HFS model provided superior performance over other tree based models. The overall results imply that PSO-HFS model could effectively be utilized to model ET_0 values quite efficiently and accurately.

Keywords:

Reference evapotranspiration, Hierarchical fuzzy systems, Fuzzy inference system, Regression tree, M5 model tree, Shannon's entropy

1. Introduction

Irrigating crops to enhance agricultural productivity essentially require sufficiently large volumes of fresh water. Water-saving through carefully managed irrigation practices can be achieved through precise quantification of evapotranspiration (ET), which is used to develop correct irrigation scheduling, determine hydrologic water balances, simulate crop yields, and allocate water resources (Kisi 2016). Being an essential component of water balance, ET plays a vital function in controlling interactions among atmosphere, soil, and the vegetation (Liu et al. 2013). The measurement of ET may be performed through experimental methods including Bowen ratio energy balance method, eddy-covariance systems, and lysimeter techniques (direct methods) (Martí et al. 2015). Alternatively, ET can be obtained by calculating potential or reference evapotranspiration (ET_0) using climatological variables. This indirect method has become popular in many parts of the world where direct measurements are not available or affordable due to complexity or costliness (Allen et al. 1998). As a universal approach of ET_0 estimation, the Penman Monteith (FAO 56 PM) method has been recognized as the widespread reference method that can be employed in arears with varying ecological and climatic circumstances with no requirement of

regional adjustments (Allen et al. 1998). FAO 56 PM equation can be utilized to estimate ET_0, which together with crop coefficient value provides an estimate of ET for a particular crop.

In recent years, artificial intelligence or machine learning based models have effectively been employed to model ET_0 in different hydrogeologic conditions. These models can map the complex and nonlinear relations between the input and output data quite effectively and accurately. Various models have been used in ET_0 modeling; among them, Artificial Neural Network (ANN) (Gocić and Arab Amiri 2021) models were the first implementation of machine learning tools to estimate ET_0. Other recent implementation of machine learning tools in ET_0 modelling includes the use of Adaptive Neuro Fuzzy Inference System (ANFIS) (Petković et al. 2020; Roy et al. 2020), Gaussian Process Regression (GPR) (Karbasi 2018), Gene-Expression Programming (GEP) (Wang et al. 2019), M5 Model Tree (M5Tree) (Kisi 2016), Multivariate Adaptive Regression Splines (MARS) (Kisi 2016), Random Forest (RF) (Wang et al. 2019; Ferreira and da Cunha 2020; Salam and Islam 2020), and Support Vector Machine (SVM) (Chia et al. 2020; Salam and Islam 2020). Generally, artificial intelligence based models have provided superior performances over the typical equations in estimating ET_0, attaining relatively better performances with similar datasets (Reis et al. 2019).

Among various machine learning algorithms, tree-based algorithms such as Random Forests, Regression Trees, and M5 Model Tree have recently been gained significant attention due to their simplicity, robustness, and capability to provide accurate predictions of ET_0 (Chen et al. 2020). On the other hand, machine learning models derived from the theory fuzzy logic have recently been utilized as an effective prediction system in various water resources management issues (Kord and Asghari Moghaddam 2014). Although an ANFIS, a variant of Fuzzy Inference System (FIS) has been successfully applied in developing ET_0 prediction models, its use is hindered by the computational burden arising from a large number of rule bases especially for problems with larger

input variables. This happens because the number of rules in a fuzzy system escalates exponentially with the quantity of variables inputted to the system. Larger rule bases make the learning and fine-tuning of the rules and membership function parameters extremely challenging. In addition, larger rule bases reduce the generalization capability of tuned fuzzy systems when there exists insufficient training data. To overcome this issue, a FIS may be represented as a tree of smaller interrelated and interconnected FIS objects known as Hierarchical Fuzzy Systems (HFS), where the predictions from the lower-level FISs are utilized as predictors to the higher-level FISs making the fuzzy tree-based HFS computationally more efficient than a single monolithic FIS object.

HFS is an improved version of decision trees that provide reliable modelling using the concept of fuzzy logic principle. Although applied quite successfully in various research domains (Zheng et al. 2019), HFS models have been given extremely little attention in the fields of hydrological and agricultural research. Few recent studies related to hydrology and water resources management also focused on the use of fuzzy logic based decision trees. For instance, Sikorska-Senoner and Seibert, (2020) employed a fuzzy logic based decision tree instead of a traditional trend analysis for quantifying the magnitudes and frequencies in the time series of floods. Wei and Hsu, (2008) performed a comparison between three types of decision trees: neural decision trees, conventional decision trees, and fuzzy decision trees to derive operating rules for a reservoir operation system. Their comparison results demonstrated the superiority of fuzzy decision trees over the other two types of decision trees. Han et al., (2002) addressed uncertainty in real time flood forecasting using fuzzy logic based fuzzy decision trees. They concluded that although fuzzy decision trees did not perform as good as the ANN models for river flow modelling in the test case, the glass box nature of fuzzy tree modelling could allow several valuable insights on the hydrological processes. As far

as the recent literature is concerned, fuzzy tree models have not yet been used in hydrological and agricultural research, especially in modelling ET_0.

Considering the importance of reliable estimates of ET_0, the purposes of this study were to: (1) assess the potentiality of PSO tuned HFS model (PSO-HFS) to predict daily ET0; (2) weigh against the prediction capability of the proposed PSO-HFS with that of two tree-based machine learning algorithms including RT, and M5 Model Tree and a fuzzy logic-based model, FIS; (3) rank the proposed models with respect to their prediction accuracies utilizing several performance evaluation indices; and (4) evaluate the generalization capability of the proposed models outside the training station using data from a test station. Accordong to the authors' understanding, this study is the first effort an evolutionary algorithm-tuned fuzzy decision tree (PSO-HFS) is employed to predict daily ET_0.

2. Materials and methods

The study proposed a fuzzy tree-based HFS model to predict daily values of ET_0 from the input-output relationships of meteorological variables and ET_0. Prediction of the proposed HFS model was then compared with that of three machine learning algorithms: a fuzzy logic-based FIS model and two tree-based models. Comparison of prediction performances was evaluated using several statistical indices within the framework of Shannon's entropy that incorporated three benefits (higher values indicate better model performance: Correlation Coefficient, Nash Sutcliffe Efficiency Coefficient, and Index of Agreement) and three cost indices (smaller values indicate better model performance: Root Mean Squared Error, Mean Absolute Error, and Median Absolute Deviation) in the decision-making process. The proposed methodology was evaluated using the daily climatic data obtained from a weather station located in the Gazipur in Bangladesh. The developed models were then validated using daily climatic data from Ishurdi meteorological

station in Bangladesh. A brief description of methodology components is presented in the subsequent subsections.

2.1. Study area and the dataset

Meteorological variables were acquired from two weather stations located in the Gazipur Sadar Upazila of the Gazipur district and Ishurdi Upazilla of the Pabna district in Bangladesh. The weather station in Gazipur is situated between 24.00°N latitude and 90.43°S longitude with an altitude of 8.4 m above the mean sea level. Meteorological variables including solar radiation, relative humidity, minimum and maximum temperatures, and wind speed were obtained for 15.5 years (from 01 January 2004 to 30 June 2019). Descriptive statistics of the meteorological variables for the training station are given in Table 1. It is perceived from Table 1 that the climatological variables demonstrated left (negative) skewness which indicates that the distribution of data for all variables had an extended left tail than the right tail. Kurtosis, on the other hand, had both positive and negative values indicating that the datasets had both "heavy-tailed" (positive values of kurtosis) and "light-tailed" (negative values of kurtosis) distributions.

[**Table 1**]

The data for the test station were acquired from 01 June 2015 to 31 December 2020 (2021 daily entries of meteorological variables and computed daily ET_0). The performance evaluation indices were calculated for the entire (2021 entries: from 01 June 2015 to 31 December 2020), first half (1021 entries: from 01 June 2015 to 17 March 2018), and the second half (1020 entries: from 18 March 2018 to 31 December 2020) of the dataset for the test station. The selection of three sets of data allows investigating a better generalization capability of the model. Descriptive statistics of the meteorological variables of the test station are presented in Table 2. The locations of the weather stations in the study areas are presented in Fig. 1.

[**Table 2**]

Meteorological variables obtained from the study areas across the period of study were utilized to estimate daily ET_0 by employing the FAO 56 PM equation. These computed daily values of ET_0 and the meteorological variables were used as outputs and inputs, respectively for the proposed HFS and other models. This indirect approach of ET_0 estimation from meteorological variables has been widely accepted in circumstances when ET_0 values are extremely hard to acquire directly (Allen et al. 1998). The FAO 56 PM equation is represented by:

$$\mathrm{ET_0} = \frac{0.408\Delta(R_n - G) + \gamma \frac{900}{T_{\mathrm{mean}} + 273} u_2 (e_s - e_a)}{\Delta + \gamma(1 + 0.34u_2)} \quad (1)$$

where, ET_0 represents reference evapotranspiration, mm d^{-1}; R_n is the net radiation at the crop surface, MJ $m^{-2}d^{-1}$; G is the heat flux density of soil, MJ $m^{-2}d^{-1}$; Δ is the slope of the saturation vapor pressure curve, $kP_a°C^{-1}$; γ is the psychometric constant, $kP_a°C^{-1}$; e_s is the saturation vapor pressure, kP_a; e_a is the actual vapor pressure, kP_a; u_2 is the wind speed at a height of 2 m, m s^{-1}; and T_{mean} is the mean air temperature at 2.0 m height, °C.

[**Fig. 1**]

For the training station (Gazipur Sadar), computed ET_0 values ranged between 0.92 and 8.02 mm d^{-1} with the mean and standard deviation values of 3.80 and 1.32 mm d^{-1}, respectively. The distribution of ET_0 time-series had an extended right tail compared to the left tail as indicated by a positive skewness value of 0.30. The negative kurtosis value of -0.67 indicates a "light-tailed" distribution for the computed ET_0 values of the train ststion. On the other hand, the mean, standard deviation, skewness, and kurtosis values of the computed ET_0 for the entire dataset of the test station were 3.67 mm d^{-1}, 1.24 mm d^{-1}, 0.28, and -0.62, respectively. For the first half of the dataset, the values were 3.57 mm d^{-1}, 1.25 mm d^{-1}, 0.35, and -0.62, respectively. The second half of the

151 dataset comprised the following values of ET_0: mean = 3.76 mm d^{-1}, standard deviation = 1.23 mm
152 d^{-1}, skewness = 0.22, kurtosis = -0.59.

153 *2.2. Proposed ET_0 prediction model: Hierarchical fuzzy systems (HFS)*

154 Fuzzy Inference Systems (FIS) are regarded as one of the most effective tools for modelling
155 dynamic and nonlinear systems with single output and multiple inputs (Takagi and Sugeno 1985;
156 Sugeno and Yasukawa 1993). However, the computational efficiency during the FIS training
157 largely relies on the quantity of inputs to the FIS system and the quantity of rule sets, which
158 generally increase exponentially as the number of input variables increases. A significant amount
159 of rule sets not only reduces the computational efficiency but also creates difficulty in the tuning
160 process of the rule base and membership function parameters. Moreover, an increased number of
161 rule bases reduces the generalization capability of tuned FISs especially in situations where the
162 amounts of training data are scarce as can be seen in many practical applications. As a solution to
163 these problems an HFS consisting of smaller interconnected FIS objects can be implemented
164 instead of a single massive FIS object with many input variables. In an HFS, the fuzzy inference
165 systems are organized in 'hierarchical tree structures' in which the predictions from the lower-
166 level FISs are employed as predictors to the higher-level FISs. With a similar number of input
167 variables, an HFS usually requires fewer computation efforts compared to a single FIS. Fuzzy tree
168 structures, based on which an HFS is constructed, can be of three major types for many practical
169 applications: (a) incremental, (b) aggregated, and (c) cascaded or combined that combines both
170 incremental and aggregated structures (Siddique and Adeli 2013). As cascaded tree structures are
171 better suited for applications with both uncorrelated and correlated input variables, a cascaded or
172 combined fuzzy tree structure is utilized in this research for constructing an HFS.

The first step of developing an HFS involves the creation of several FIS objects using the available input variables ranked based on their correlations with the output variable (ET_0). Both positively and negatively correlated input attributes were used to incorporate both the positive and negative impacts of input attributes on the output (ET_0) for prediction. Next, in the second step, the input attributes were paired concerning their ranks to create individual FIS object as follows:

- fis1: Maximum Temperature and Relative Humidity
- fis2: Wind Speed and Sunshine Duration
- fis3: Minimum Temperature and Sunshine Duration

[**Fig. 2**]

Then, the HFS as shown in Fig. 2, was constructed using the principle of FIS tree structure (Mathworks 2021). The constructed HFS had five two-input and one-output FIS objects (fis1, fis2, fis3, fis4, and fis5 in Fig. 2) of which the first three FISs (fis1, fis2 and fis3) received the ranked input attributes directly and produced intermediate predictions of ET_0. The intermediate ET_0 values were integrated utilizing the remaining two FISs (fis4 and fis5).

2.3. Other prediction models

2.3.1. Fuzzy inference system (FIS)

The underlying principles of FIS are derived from fuzzy set theory that has received considerable attention in recent years. FISs have successfully been applied as a reliable computing framework in various research areas (Jang et al. 1997). They have been regarded as effective prediction tools for modelling nonlinear processes due to their capability of accurately mapping of the relationships (usually nonlinear) between input and output variables (Takagi and Sugeno 1985; Sugeno and Yasukawa 1993). A Sugeno Sugeno-type FIS (Sugeno, 1985), also known as a Takagi-Sugeno-Kang FIS, is particularly better fitted for nonlinear system modelling. A Sugeno FIS builds input-

196 output relationships through interpolating the outputs from multiple linear models. The basic
197 structure of a Sugeno FIS consists of a rule base, a database, and a reasoning mechanism. The
198 working principle of a basic FIS with three inputs, one output, and four rules is illustrated in a
199 block diagram as shown in Fig. 3.

200 [**Fig. 3**]

201 Rule bases of an FIS consist of fuzzy if-then rules, the database determines the types and numbers
202 of MFs utilized in fuzzy rules, and finally, the reasoning mechanism accomplishes the fuzzy
203 inference process (Jang et al. 1997). Several fuzzy if-then rules are utilized in a fuzzy inference
204 process for producing a nonlinear mapping of input and output variables. A fuzzy rule consists of
205 two parts: (a) antecedent part of any rule specifies a fuzzy region within the input variable space,
206 and (b) consequent part specifies a fuzzy region within the output variable space. A Sugeno-type
207 FIS introduced in 1985 (Sugeno 1985) was developed and utilized in this effort. The input and
208 output MFs of the utilized Sugeno FIS were Gaussian and linear, respectively.

209 2.3.2. M5 model tree

210 The development of M5 model trees is based on the principles of the M5 method (Quinlan 1992).
211 This method builds single trees corresponding to a method called 'M5', which makes use of the
212 'Standard Deviation Reduction' criterion. Model trees (MT) are combinations of traditional
213 regression trees which possess linear regression functions at the leaf nodes. Pruning and smoothing
214 operators determine the contents of a leaf node for a MT, which is nothing but a regression tree
215 without 'pruning' and 'smoothing' operations. MTs (Quinlan 1992) are machine learning
216 algorithms that have demonstrated their predictive capabilities in various research domains
217 (Bhattacharya and Solomatine 2005). MTs are 'inverted trees', i.e., root nodes are situated at the
218 upper portion of the tree whereas the bottom portion of the tree contains the leaves.

MTs and regression trees are the variants of Decision Trees (DT) that have been established for solving regression tasks (Quinlan 1992). However, MTs differ from regression trees: while MTs generate linear models at their leaves, the regression trees yield a constant value at their leaves. The linear models developed at the leaves are used to contain input-output relationships, which are then utilized to predict outputs for a given set of data. MTs are more efficient than regression trees in handling large datasets and producing more accurate predictions. M5 MT utilizes 'divide-and-conquer' method that allows dividing the entire data space into smaller data sub-spaces (Bhattacharya and Solomatine 2005). In this approach, the input parameter space is narrowed down to several subspaces each of which represents a linear regression model. This unique data splitting procedure enables M5 MT to produce a hierarchial model tree that contains splitting rules in its non-terminal nodes and has expert models in its leaves.

A MATLAB toolbox "M5PrimeLab" (Jekabsons 2016) was employed to built M5 model trees for predicting daily reference ET_0 values with various climatic variables as inputs and ET_0 values as outputs.

2.3.3. Regression tree

Regression trees (RT) are decision trees that build simple, flexible, and easily interpretable models developed using input-output training patterns. RTs are associated with the principle of 'Classification and Regression Tree (CART)' algorithm (Breiman et al. 1984; Krzywinski and Altman 2017). The CART algorithm follows three major stepwise procedures in building models: (a) building a complex tree, (b) pruning, and (c) selecting an optimal subtree. In the first step, a complex full tree with several terminal nodes is built using a binary split procedure. The complex tree built in the first step is pruned in the second step to prevent or at least reduce model overfitting. In the third step, an optimal subtree is selected by the CART algorithm to ensure the quality of

prediction for new samples. The developed RTs deliver a predicted response through the following decisions from the beginning node (root node) to the leaf node within the tree. The leaf node of an RT contains the responses or outputs. The RT-based ET_0 prediction models were developed in the MATLAB environment.

2.4. Input-output training patterns for ET_0 prediction models

The meteorological variables and the estimated ET_0 formed the input-output datasets for the proposed ET_0 prediction models. The dataset of the training station contains 5660 daily entries (from 01 January 2004 to 30 June 2019) of meteorological variables and estimated ET_0 values. The entire dataset of 5660 entries was separated into training, validation, and test sets: first 80% of the total data (4528 entries: from 01 January 2004 to 24 May 2016) was used to train and validate the proposed models whereas the last 20% (1132 entries: from 25 May 2016 to 30 June 2019) was used to test the developed models. The first 80% of the sequential data were randomized to minimize the effect of trends during the model training and validation process. The randomized data were then split into two equal-sized datasets for training (first 40%) and validation (remaining 40%) sets. It is noted that the test set (last 20% of the entire dataset) was kept in sequence as this dataset was used to test the developed models for the actual nature of data. This technique of data partitioning allows better performance evaluation for the developed models (Francone 2001). For performance evaluation, numerous statistical indices were computed on the test dataset.

3. Parameter tuning of HFS: Particle swarm optimization

A parameter tuning approach was adopted to achieve optimum performance of the constructed HFS. Both the rule bases and input-output Membership Functions (MF) were tuned in two subsequent phases. In the first phase, learning of the rule bases was accomplished while input and output MF parameters were kept constant. After learning the new rules through the first phase, the

parameters of the input-output MF, as well as the learned rules, were tuned simultaneously in the second phase. To achieve computational efficiency in the parameter tuning process, the tuned rule base obtained from the first phase was used as the initial condition for the second phase. This allows a fast parameter tuning process and quick convergence to global optima. Particle Swarm Optimization (PSO) has recently gained popularity due to the possession of many advantageous characteristics such as it has simple structure, robust maneuverability, and easy realization that facilitates the training of various intelligent models. Therefore, this study utilized PSO in both phases of parameter tuning to obtain optimal parameter values of the constructed HFS.

The PSO (Kennedy and Eberhart 1995), a swarm-based stochastic search algorithm, is encouraged by communal and psychological principles. The PSO is associated with the principles of swarm intellect, which feigns the communal behavior of predation commonly observed in fish schooling or bird flocking. In PSO, every single particle is regarded as a 'feasible solution' over the entire search space for a given optimization problem. On the other hand, the flight behavior of particles is regarded as the search method for all individuals within a community. In PSO, the dynamic update of the velocity of particles is determined by the past optimal location of the particle and the population within a swarm. In PSO, the particle's objective function values are the corresponding fitness values. These fitness values determine the optimum particle position. The fitness values are also used to update the past most favorable location of the particles and the optimal location of the swarm population. The control parameters of the PSO algorithm determine the convergence of particle trajectories. Convergence of the PSO algorithm is attained through maintaining a memory of standalone best fitness values of each particle, locating the global best particle, and bringing up to date the location and velocity of all particles. If the convergence is not attained, the iterative

process repeats till the optimization problem reaches to its optimal solution or the user defined maximum quantity of iterations is attained.

4. Implementation of the proposed HFS to model ET_0

In developing the proposed models, ET_0 was considered as the target variable whereas the meteorological variables were used as the inputs. The inputs to and outputs from the HFS can be represented in the generalized form as:

$$Reference\ evapotranspiration, ET_0 = f(meteorological\ variables) \quad (2)$$

Determining the optimal parameter values which have a significant impact on the output variable is the most important step in developing predictive models. Parameter tuning was performed using a swarm-based optimization algorithm, PSO described earlier in the previous section (section 3: Parameter tuning of HFS: Particle swarm optimization). To further improve the HFS model's accuracy, all tunable parameters (rule bases and parameters of both input and output MFs) were optimized using the PSO algorithm. The parameters of the PSO algorithm were selected upon several trials concerning a tradeoff between prediction precision and computational efficiency.

Eventually, the input-output datasets used to construct the prediction models were split into train, validation, and test sets. Additionally, FIS, M5 Model Tree, and RT-based ET_0 prediction models were also developed solely for comparison purposes. Nonlinear mapping of inputs and outputs for a typical ET_0 prediction modelling approach can be schematically represented by Fig. 4.

[**Fig. 4**]

5. Ranking of models: Shannon's entropy

Shannon's entropy (Shannon 1948) was applied to assign weights to individual ET_0 prediction models which were ranked according to the weights assigned to them. Shannon's entropy

incorporates a set of benefit (the higher values indicate better model accuracy) and cost (the lower values indicate better model accuracy) performance evaluation indices. The detailed calculation steps of Shannon's entropy can be found in Roy et al. (2020), and are not repeated here.

6. Performance evaluation criteria

The proposed modelling approach was evaluated with several performance indicators as follows:

Root Mean Squared Error, RMSE:

$$RMSE = \frac{\sqrt{\frac{1}{n}\sum_{i=1}^{n}\left(ET_{0_i}^{A} - ET_{0_i}^{P}\right)^2}}{\overline{ET_0^{A}}} \tag{3}$$

Normalized RMSE, NRMSE:

$$NRMSE = \frac{RMSE}{\overline{ET_0^{A}}} \tag{4}$$

Accuracy:

$$Acc = 1 - abs\left(mean\frac{ET_{0_i}^{P} - ET_{0_i}^{A}}{ET_{0_i}^{A}}\right) \tag{5}$$

Mean Bias Error (MBE):

$$MBE = \frac{1}{n}\sum\left(ET_{0_i}^{P} - ET_{0_i}^{A}\right) \tag{6}$$

Nash-Sutcliffe Efficiency Coefficient (NS):

$$NS = 1 - \frac{\sum_{i=1}^{n}\left(ET_{0_i}^{A} - ET_{0_i}^{P}\right)^2}{\sum_{i=1}^{n}\left(ET_{0_i}^{A} - \overline{ET_0^{A}}\right)^2} \tag{7}$$

Willmott's Index of Agreement (IOA):

$$d = 1 - \frac{\sum_{i=1}^{n}\left(ET_{0_i}{}^{A} - ET_{0_i}{}^{P}\right)^2}{\sum_{i=1}^{n}\left(\left|ET_{0_i}{}^{P} - \overline{ET_0{}^{A}}\right|\left|ET_{0_i}{}^{A} - \overline{ET_0{}^{A}}\right|\right)^2} \quad (8)$$

Mean Absolute Error, MAE

$$MAE = \text{Average}\left[\left|ET_{0_i}{}^{A} - ET_{0_i}{}^{P}\right|\right] \quad (9)$$

Median Absolute Deviation, MAD

$$MAD\left(ET_{0_i}{}^{A}, ET_{0_i}{}^{P}\right) = median\left(\left|ET_{0_1}{}^{A} - ET_{0_1}{}^{P}\right|, \left|ET_{0_2}{}^{A} - ET_{0_2}{}^{P}\right|, \ldots, \left|ET_{0_n}{}^{A} - ET_{0_n}{}^{P}\right|\right) \quad for\ i = 1,2,\ldots,n \quad (10)$$

Correlation Coefficient (R):

$$R = \frac{\sum_{i=1}^{n}\left(ET_{0_i}{}^{A} - \overline{ET_0{}^{A}}\right)\left(ET_{0_i}{}^{A} - \overline{ET_0{}^{P}}\right)}{\sqrt{\sum_{i=1}^{n}\left(ET_{0_i}{}^{A} - \overline{ET_0{}^{A}}\right)^2}\sqrt{\sum_{i=1}^{n}\left(ET_{0_i}{}^{P} - \overline{ET_0{}^{P}}\right)^2}} \quad (11)$$

where, $ET_{0_i}{}^{A}$ and $ET_{0_i}{}^{P}$ are the FAO 56 PM estimated and model predicted ET_0 values for the i^{th} data points of the dataset, respectively; $\overline{ET_0{}^{A}}$ and $\overline{ET_0{}^{P}}$ are the mean of the FAO 56 PM estimated and model predicted ET_0 values, respectively; n is the number of data points in the dataset.

7. Results and discussion

The values of FAO 56 PM estimated ET_0 were considered as the benchmark for evaluating the performances of the proposed HFS, and other models (FIS, M5 Model Tree, and RT) developed for comparison purposes. Ten statistical performance assessment indices were computed for both the calibration (Training and Validation datasets) and testing (applied dataset) phases of model building. Performance assessment indices were calculated on the FAO 56 PM estimated and model predicted ET_0 values. Performances of the developed models to the computed performance indices for the calibration and testing phases are presented in the subsequent paragraphs.

7.1. Performance of the HFS during the training phase

The training phase of model building is regarded as the most important step in the development of any prediction model. To prevent model over-or underfitting, training performance is compared with the validation performance using the validation data. Training and validation phases were performed simultaneously, and several evaluation indices were calculated on the model predicted and FAO 56 PM estimated ET_0 values. Performances of the Proposed HFS and other tree-based models during training and validation stages are shown in Table 3. It is evidenced from Table 3 that all performance indices showed a reasonably good performance of the proposed HFS model during training and validation stages as evidenced by the negligible difference in values of the performance evaluation indices between these two phases.

[**Table 3**]

Although not as accurate as the proposed HFS model, the FIS-based model performed equally well during the training and validation phases (Table 3). Training performances of RT and M5 Model Tree were observed relatively better than their validation performances especially on the cost indices (MAD, MAE, MAPRE, RMSE, and NRMSE) as shown in Table 3. However, their performances on benefit indices (e.g., accuracy, IOA, NS, and R) were found to be almost similar which indicates reasonably decent performance on the benefit indices. Overall, the training and validation performances of the proposed HFS model were obtained superior to the other tree-based models. Nevertheless, although performed differently on different performance indices as well as on the training and validation phases, all models presented in Table 3 produced quite acceptable results in the context of prediction modelling.

Although RT and M5 Model Tree suffered slightly from model overfitting as evidenced by the results obtained from the cost indices, the models produced satisfactory results concerning the

benefit indices. This is also acceptable because prediction models often show contradictory performances, i.e., one model may be deemed suitable based on the RMSE criterion whereas the other model may be a good performer based on the R criterion (Müller and Piché 2011; Roy and Datta 2019, 2020). This conflicting nature of the prediction models necessitates the incorporation of several performance evaluation indices instead of few indices within a framework of a decision theory for judging the performance of any prediction model. A decision theory incorporating Shannon's entropy based weighting system was applied to judge the performance and to rank the developed models for the test performances of the trained and validated models (Subsection 7.3: Ranking of the developed ET_0 prediction models).

7.2. Performance of the HFS during the testing phase

The proposed HFS and other tree-based models were further tested using the test data which were used neither to train nor to validate the models, i.e., the models were tested using data from outside the training and validation datasets. The performances during the testing phase (with applied dataset) computed on the estimated FAO 56 PM and model-predicted (calibrated and validated) ET_0 values using several performance evaluation indices are presented in Table 4.

[**Table 4**]

As the results indicate, the models performed equally well when compared to the training and validation phases. It is observed from Table 3 that although the performances were slightly poor during the applied phase when compared to the calibration and validation phases, the model performance during the applied phase was excellent in the context of prediction modelling. The applied results produced accuracy > 0.97, IOA > 0.99, NS > 0.99, R > 0.95, MAD<0.2, MAE<0.3, MAPRE<8%, and NRMSE<0.1 which indicate an excellent model performance. Models' performance is deemed excellent when the NS statistic value is greater than 0.8 (Gupta et al. 1999)

379 suggesting an efficient performance of the developed models. Moreover, the NRMSE (or scatter
380 index) values in the applied phase were 0.052 and 0.093, respectively for the best (HFS) and the
381 worst (RT) model. These NRMSE values also illustrate the excellent performance of the developed
382 models based on the criteria set in Heinemann et al., (2012) and in Li et al., (2013). According to
383 them, model performance is said to be excellent when NRMSE value is lower than 0.1, good when
384 NRMSE value is between 0.1 and 0.2, fair when NRMSE value is between 0.2 and 0.3, poor when
385 NRMSE is greater than 0.3. In general, model performance for all the developed models was
386 satisfactory as indicated by the lower values of MAD, MAE, MAPRE, and NRMSE together with
387 higher values of accuracy, IOA, NS, and R.

388 The model performances were also evaluated based on scatter and regression plots presented in
389 Figs. 5 and 6. ET_0 estimates of the four modelling approaches with the benchmark FAO 56 PM
390 method during the test period were illustrated in Fig. 5. As can be observed, the HFS predictions
391 were nearer to the FAO 56 PM estimated ET_0 values than the FIS and RT models. On the other
392 hand, fluctuations of model predictions were remarkably close to each other in the case of the HFS
393 and M5 Model Tree. This confirms the calculated performance evaluation indices presented in
394 Table 3.

395 [**Fig. 5**]

396 Comparison of the regression plots obtained from the model predictions and FAO 56 PM estimates
397 for the test dataset is illustrated in Fig. 6. It is apparent from the regression plots that the HFS had
398 fewer scattered predictions compared to the FIS and RT models, and was closely followed by the
399 M5 Model Tree. Regression plots confirmed the superior performance of the HFS model over the
400 FIS, RT, and M5 Model Tree.

401 [**Fig. 6**]

Prediction accuracies of the proposed HFS and three other tree-based models presented as box plots of absolute errors (Fig. 7) reveal that the PSO tuned HFS model outperformed other prediction models and that the accuracy of prediction for the M5 Model tree was better than FIS and RT models. It is worth mentioning that the prediction accuracy of the M5 Model Tree was equally well with the HFS model accuracy. However, the M5 Model Tree had more high magnitude absolute error values when compared to the HFS model. Therefore, it is evidenced that the HFS model is considered as the superior performer, among others.

[**Fig. 7**]

Prediction performances of the proposed HFS and other tree-based models were also evaluated using spider plots, also termed as 'radar' (Rankin et al., 2008), which can assess the performance of multifunctional systems. In a spider plot, relevant performance indices are chosen and assigned to an axis on a multidimensional plot. Displaying relevant data, a spider plot can be employed to evaluate the performance of any multifunctional entity, including performances of several prediction models on a particular performance evaluation index calculated using the actual and model-predicted data. In this effort, spider plots were drawn to illustrate performances of the developed prediction models on two benefits (Accuracy and R) and four cost indices (RMSE, MAE, MAD, MBE). The results are presented in Fig. 8 which demonstrate the superiority of the HFS model over the M5 Model Tree, FIS, and RT.

[**Fig. 8**]

7.3. Ranking of the developed ET_0 prediction models

It is an apparent and well-established fact that prediction models behave differently in terms of prediction accuracies when different performance evaluation criteria are used to compute the

prediction performances (Roy et al., 2020). This contrasting behavior of prediction models needs to be resolved to provide an unbiased suitability of an individual model. To resolve this contradictory behavior of models, Shannon's entropy-based decision theory was applied to provide ranking of the considered prediction models. This ranking approach made use of six performance indices, three of them were benefit indices (the higher values designate better model accuracy: R, NS, and IOA) while the remaining three were cost indices (the lower values designate better model accuracy: RMSE, MAE, and MAD). These benefit and cost indices were incorporated in calculating the weights for individual prediction models. The entropy weights calculated using Shannon's entropy are presented in Fig. 9.

[**Fig. 9**]

It is apparent from Fig. 9 that Shannon's entropy-based decision theory determined that the HFS (entropy weight = 0.93) model had superior performance, followed by the M5 Model Tree (entropy weight = 0.90), FIS (entropy weight = 0.77), and RT (entropy weight = 0.74) models. It can, therefore, be concluded that the PSO tuned HFS model achieved higher accuracy than the other tree-based prediction models considered in this effort.

8. Generalization of developed models for a new unseen test dataset

The HFS and other tree-based models developed at the training station (Gazipur Sadar) were validated using meteorological data obtained from a test station (Ishurdi ststion). Three distinct sets of data of the test station were inputted to the developed models for predicting daily ET0, which were then compared with the estimated ET_0 and differrnt performance evaluation indices were computed using the model predicted and FAO 56 PM estimated ET_0 values. The performance evaluation results in terms of various statistical indices are shown in Table 5. As the results indicate, the models performed equally well when compared to the results of the training station.

447 The model performances were satisfactory concerning the computed statistical indices: the model
448 produced higher values of accuracy, NS, IOA, and R as well as lower values of RMSE, NRMSE,
449 and MBE for all three datasets.

450 [**Table 5**]

451 **9. Conclusion**

452 The potential of the PSO tuned HFS modelling approach for the prediction of ET_0 using climatic
453 variables was explored in this research. The study revealed that modelling of daily ET_0 can
454 efficiently be predicted using the Fuzzy logic-based HFS model, specifically when TMF is
455 employed to develop the Sugeno type FIS for the construction of HFS. Five input attributes
456 (climatic variables) such as solar radiation, relative humidity, minimum and maximum
457 temperatures, and wind speed were utilized to predict the daily ET_0. The HFS was constructed
458 from five FIS objects built using the ranked input attributes (correlations of the input attributes
459 with the output attribute, ET_0). The input-output MFs and the rule bases of the constructed HFS
460 were then tuned in two steps with PSO that provided fast convergence of the parameter tuning
461 process for the training dataset. The train and validation with the dataset of the train station
462 revealed that the developed HFS adequately mapped the input-output patterns of the train Station
463 dataset. Therefore, an HFS can effectively be applied in predicting ET_0 with climatic variables as
464 inputs. Nevertheless, it is of crucial importance to test the developed HFS model's performance
465 outside the training and validation dataset. To test the reliability of the HFS model in predicting
466 ET_0 for the unseen test dataset (used neither to train nor validate the developed HFS), the
467 developed HFS model was employed to predict ET_0 for the test dataset. Results revealed the
468 potentiality of the HFS model in accurate and reliable prediction of ET_0 for the test dataset. The

proposed modelling tool provides a promising approach for ET_0 estimation in sub-tropical climates.

The study applied data from one weather station and the developed models were tested for the unseen test dataset. It is worthwhile to assess the usability of the proposed HFS modelling approach by including weather stations with varying climatic zones. Future research may be directed towards exploring and comparing other bio-inspired optimization algorithms for the parameter tuning process of the HFS models.

Declarations

Funding: This research did not receive any specific grant from funding agencies in the public, commercial, or not-for-profit sectors.

Conflicts of interest/Competing interests: The authors declare that there is no conflict of interest.

Availability of data and material**:** Datasets and other materials are available with the authors, and may be accessible at any time upon request.

Code availability: MATLAB codes are available with the first author.

References

Allen RG, Pereira LS, Raes D, Smith M (1998) Crop evapotranspiration— guidelines for computing crop water requirements. FAO Irrig Drain Pap No 56, Rome

Bhattacharya B, Solomatine DP (2005) Neural networks and M5 model trees in modelling water level–discharge relationship. Neurocomputing 63:381–396. https://doi.org/https://doi.org/10.1016/j.neucom.2004.04.016

Breiman L, Friedman JH, Olshen RA, Stone CJ (1984) Classification and regression trees. Wadsworth International, CA, USA.

Chen H, Huang JJ, McBean E (2020) Partitioning of daily evapotranspiration using a modified shuttleworth-wallace model, random Forest and support vector regression, for a cabbage farmland. Agric Water Manag 228:105923. https://doi.org/https://doi.org/10.1016/j.agwat.2019.105923

Chia MY, Huang YF, Koo CH (2020) Support vector machine enhanced empirical reference evapotranspirationestimation with limitedmeteorological parameters. Comput Electron Agric 175:105577. https://doi.org/https://doi.org/10.1016/j.compag.2020.105577

Ferreira LB, da Cunha FF (2020) New approach to estimate daily reference evapotranspiration based on hourly temperature and relative humidity using machine learning and deep learning. Agric Water Manag 234:106113. https://doi.org/https://doi.org/10.1016/j.agwat.2020.106113

Ferreira LB, da Cunha FF, de Oliveira RA, Fernandes Filho EI (2019) Estimation of reference evapotranspiration in Brazil with limited meteorological data using ANN and SVM – A new approach. J Hydrol 572:556–570. https://doi.org/https://doi.org/10.1016/j.jhydrol.2019.03.028

Francone FD (2001) Owner's manual: Fast genetic programming based on AIMLearning technology

Gocić M, Arab Amiri M (2021) Reference evapotranspiration prediction using neural networks and optimum time lags. Water Resour Manag 35:1913–1926. https://doi.org/10.1007/s11269-021-02820-8

Gupta HV, Sorooshian S, Yapo PO (1999) Status of automatic calibration for hydrologic models: Comparison with multilevel expert calibration. J Hydrol Eng 4:135–143.

https://doi.org/10.1061/(ASCE)1084-0699(1999)4:2(135)

Han D, Cluckie ID, Karbassioun D, et al (2002) River flow modelling using fuzzy decision trees. Water Resour Manag 16:431–445. https://doi.org/10.1023/A:1022251422280

Heinemann AB, Oort PAV, Fernandes DS, Maia A (2012) Sensitivity of APSIM/ORYZA model due to estimation errors in solar radiation. Bragantia 71:572–582

Jang J-SR, Sun C-T, Mizutani E (1997) Neuro-fuzzy and soft computing: A computational approach to learning and machine intelligence. Prentice-Hall, Upper Saddle River, New Jersey

Jekabsons G (2016) M5PrimeLab: M5' regression tree, model tree, and tree ensemble toolbox for Matlab/Octave

Karbasi M (2018) Forecasting of multi-step ahead reference evapotranspiration using wavelet-Gaussian process regression model. Water Resour Manag 32:1035–1052. https://doi.org/10.1007/s11269-017-1853-9

Kennedy J, Eberhart R (1995) Particle swarm optimization. In: Proceedings of ICNN'95 - International Conference on Neural Networks. pp 1942–1948 vol.4

Kisi O (2016) Modeling reference evapotranspiration using three different heuristic regression approaches. Agric Water Manag 169:162–172. https://doi.org/https://doi.org/10.1016/j.agwat.2016.02.026

Kord M, Asghari Moghaddam A (2014) Spatial analysis of Ardabil plain aquifer potable groundwater using fuzzy logic. J King Saud Univ - Sci 26:129–140. https://doi.org/https://doi.org/10.1016/j.jksus.2013.09.004

Krzywinski M, Altman N (2017) Classification and regression trees. Nat Methods 14:757–758.

https://doi.org/10.1038/nmeth.4370

Li M-F, Tang X-P, Wu W, Liu H-B (2013) General models for estimating daily global solar radiation for different solar radiation zones in mainland China. Energy Convers Manag 70:139–148. https://doi.org/https://doi.org/10.1016/j.enconman.2013.03.004

Liu SM, Xu ZW, Zhu ZL, et al (2013) Measurements of evapotranspiration from eddy-covariance systems and large aperture scintillometers in the Hai River Basin, China. J Hydrol 487:24–38. https://doi.org/https://doi.org/10.1016/j.jhydrol.2013.02.025

Martí P, González-Altozano P, López-Urrea R, et al (2015) Modeling reference evapotranspiration with calculated targets. Assessment and implications. Agric Water Manag 149:81–90. https://doi.org/https://doi.org/10.1016/j.agwat.2014.10.028

Mathworks (2021) Technical documentation. In: Fuzzy trees. https://au.mathworks.com/help/fuzzy/fuzzy-trees.html. Accessed 5 May 2021

Müller J, Piché R (2011) Mixture surrogate models based on Dempster-Shafer theory for global optimization problems. J Glob Optim 51:79–104. https://doi.org/10.1007/s10898-010-9620-y

Petković B, Petković D, Kuzman B, et al (2020) Neuro-fuzzy estimation of reference crop evapotranspiration by neuro fuzzy logic based on weather conditions. Comput Electron Agric 173:105358. https://doi.org/https://doi.org/10.1016/j.compag.2020.105358

Quinlan JR (1992) Learning with continuous classes. In: Proceedings of Australian Joint Conference on Artificial Intelligence. Hobart 16-18 November, pp 343–348

Reis MM, da Silva AJ, Zullo Junior J, et al (2019) Empirical and learning machine approaches to estimating reference evapotranspiration based on temperature data. Comput Electron Agric

165:104937. https://doi.org/https://doi.org/10.1016/j.compag.2019.104937

Roy DK, Barzegar R, Quilty J, Adamowski J (2020) Using ensembles of adaptive neuro-fuzzy inference system and optimization algorithms to predict reference evapotranspiration in subtropical climatic zones. J Hydrol 591:125509. https://doi.org/https://doi.org/10.1016/j.jhydrol.2020.125509

Roy DK, Datta B (2019) An ensemble meta-modelling approach using the Dempster-Shafer theory of evidence for developing saltwater intrusion management strategies in coastal aquifers. Water Resour Manag 33:775–795. https://doi.org/10.1007/s11269-018-2142-y

Roy DK, Datta B (2020) Saltwater intrusion prediction in coastal aquifers utilizing a weighted-average heterogeneous ensemble of prediction models based on Dempster-Shafer theory of evidence. Hydrol Sci J 1–13. https://doi.org/10.1080/02626667.2020.1749764

Salam R, Islam ARMT (2020) Potential of RT, bagging and RS ensemble learning algorithms for reference evapotranspiration prediction using climatic data-limited humid region in Bangladesh. J Hydrol 590:125241. https://doi.org/https://doi.org/10.1016/j.jhydrol.2020.125241

Shannon CE (1948) A mathematical theory of communication. Bell Syst Tech J 27:379–423. https://doi.org/10.1002/j.1538-7305.1948.tb01338.x

Siddique N, Adeli H (2013) Computational intelligence: Synergies of fuzzy logic, neural networks and evolutionary computing. Wiley, Hoboken, NJ

Sikorska-Senoner AE, Seibert J (2020) Flood-type trend analysis for alpine catchments. Hydrol Sci J 65:1281–1299. https://doi.org/10.1080/02626667.2020.1749761

Sugeno M (1985) Industrial applications of fuzzy control. Elsevier Science Inc.655 Avenue of

the Americas New York, NYUnited States

Sugeno M, Yasukawa T (1993) A fuzzy-logic-based approach to qualitative modeling. IEEE Trans Fuzzy Syst 1:7. https://doi.org/10.1109/TFUZZ.1993.390281

Takagi T, Sugeno M (1985) Fuzzy identification of systems and its applications to modeling and control. IEEE Trans Syst Man Cybern SMC-15:116–132. https://doi.org/10.1109/TSMC.1985.6313399

Wang S, Lian J, Peng Y, et al (2019) Generalized reference evapotranspiration models with limited climatic data based on random forest and gene expression programming in Guangxi, China. Agric Water Manag 221:220–230. https://doi.org/https://doi.org/10.1016/j.agwat.2019.03.027

Wei C-C, Hsu N-S (2008) Derived operating rules for a reservoir operation system: Comparison of decision trees, neural decision trees and fuzzy decision trees. Water Resour Res 44:2428. https://doi.org/10.1029/2006WR005792

Zheng H, He J, Zhang Y, et al (2019) A general model for fuzzy decision tree and fuzzy random forest. Comput Intell 35:310–335. https://doi.org/https://doi.org/10.1111/coin.12195

602 **Table 1** Statistical metrices of climatological variables obtained from an automatic weather station
603 located in Gazipur Sadar Upazilla, Bangladesh

Variables	Mean	Standard deviation	Skewness	Kurtosis
Minimum temperature, °C	21.17	5.64	-0.63	-0.88
Maximum temperature, °C	30.93	3.92	-1.10	2.11
Relative humidity, %	80.22	8.20	-0.63	0.75
Wind speed, km/d	241.15	90.69	-0.06	-1.32
Sunshine duration, h	5.54	3.09	-0.40	-1.04

604

605

606 **Table 2** Descriptive statistics of meteorological variables for the test station (Ishurdi station),
607 Bangladesh

Variables	Mean	Standard deviation	Skewness	Kurtosis
Entire dataset				
Minimum temperature, °C	21.37	5.98	-0.73	-0.76
Maximum temperature, °C	31.46	4.16	-0.83	0.28
Relative humidity, %	78.89	12.18	-1.23	1.93
Wind speed, $\mathbf{m\ s^{-1}}$	1.43	0.23	0.07	0.22
Sunshine duration, h	5.90	3.19	-0.41	-0.71
First half data				
Minimum temperature, °C	21.06	6.08	-0.65	-0.92
Maximum temperature, °C	31.27	4.21	-0.71	0.26
Relative humidity, %	80.06	11.30	-1.24	2.25
Wind speed, $\mathbf{m\ s^{-1}}$	1.43	0.23	0.06	0.35
Sunshine duration, h	5.75	3.18	-0.42	-0.98
Second half data				
Minimum temperature, °C	21.69	5.87	-0.83	-0.56
Maximum temperature, °C	31.66	4.11	-0.95	0.35
Relative humidity, %	77.71	12.89	-1.18	1.54
Wind speed, $\mathbf{m\ s^{-1}}$	1.44	0.23	0.09	0.08
Sunshine duration, h	6.05	3.19	-0.39	-0.44

608

609

610

611

612

613

614

615 **Table 3** Performances of HFS and other tree-based models on the training and validation dataset
616

Performance Indices	HFS		FIS		RT		M5 Model Tree	
	Train	Validation	Train	Validation	Train	Validation	Train	Validation
Accuracy	0.996	0.994	0.996	0.996	0.998	0.989	0.999	0.996
IOA	0.995	0.993	0.986	0.985	0.996	0.985	0.998	0.993
MAD, mm d^{-1}	0.071	0.072	0.117	0.117	0.056	0.111	0.045	0.065
MAE, mm d^{-1}	0.148	0.149	0.243	0.246	0.120	0.237	0.093	0.150
MAPRE, %	4.374	4.453	8.228	8.332	3.441	6.800	2.735	4.384
MBE	-0.003	0.010	0.000	0.022	0.000	0.023	0.000	0.004
NRMSE	0.052	0.056	0.082	0.084	0.043	0.084	0.033	0.059
NS	0.979	0.974	0.947	0.943	0.986	0.943	0.991	0.972
R	0.989	0.987	0.973	0.971	0.993	0.971	0.996	0.986
RMSE, mm d^{-1}	0.199	0.211	0.316	0.316	0.164	0.316	0.127	0.221

617 *HFS = Hierarchal Fuzzy Systems, FIS = Fuzzy Inference System, RT = Regression Tree, IOA = Willmott's Index of Agreement, MAD =
618 Median Absolute Deviation, MAE = Mean Absolute Error, MAPRE = Mean Absolute Percentage Relative Error, MBE = Mean Bias Error,
619 NRMSE = Normalized RMSE, NS = Nash Sutcliffe Efficiency Coefficient, R = Correlation Coefficient, RMSE = Root Mean Squared Error

620

621

622 **Table 4** Performances of HFS and other tree-based models on the applied dataset

Performance Indices	HFS	FIS	RT	M5 Model Tree
Accuracy	0.989	0.977	0.981	0.987
IOA	0.999	0.999	0.998	0.999
MAD, mm d^{-1}	0.068	0.114	0.116	0.066
MAE, mm d^{-1}	0.148	0.225	0.255	0.158
MAPRE, %	4.420	7.072	7.344	4.657
MBE	0.029	0.064	0.050	0.038
NRMSE	0.052	0.075	0.093	0.063
NS	0.998	0.995	0.992	0.996
R	0.987	0.973	0.958	0.980
RMSE, mm d^{-1}	0.197	0.288	0.355	0.240

623

624

625

626

627

628

629

630

631 **Table 5** Performance of the HFS and other tree-based models using climatic data from test station
632 (Ishurdi station)

Indices	Entire dataset				First half data				Second half data			
	HFS	FIS	RT	M5	HFS	FIS	RT	M5	HFS	FIS	RT	M5
Accuracy	0.90	0.87	0.89	0.86	0.90	0.86	0.89	0.87	0.90	0.88	0.88	0.85
IOA	0.94	0.93	0.83	0.85	0.95	0.93	0.84	0.87	0.93	0.92	0.81	0.84
MAD, mm d^{-1}	0.27	0.27	0.37	0.41	0.26	0.29	0.32	0.38	0.28	0.26	0.40	0.43
MAE, mm d^{-1}	0.46	0.58	0.68	0.66	0.44	0.56	0.64	0.62	0.49	0.60	0.72	0.70
MAPRE, %	12.34	17.04	16.52	16.19	12.04	17.06	15.94	15.55	12.64	17.02	17.09	16.82
MBE	-0.38	-0.44	-0.53	-0.61	-0.37	-0.46	-0.50	-0.56	-0.35	-0.38	-0.50	-0.59
NRMSE	0.16	0.19	0.24	0.23	0.16	0.19	0.24	0.23	0.16	0.18	0.25	0.23
NS	0.77	0.70	0.48	0.53	0.79	0.71	0.52	0.58	0.75	0.68	0.43	0.48
R	0.93	0.91	0.82	0.90	0.94	0.92	0.83	0.90	0.92	0.90	0.80	0.90
RMSE, mm d^{-1}	0.59	0.68	0.90	0.85	0.57	0.67	0.87	0.81	0.62	0.69	0.93	0.88

633

634

635

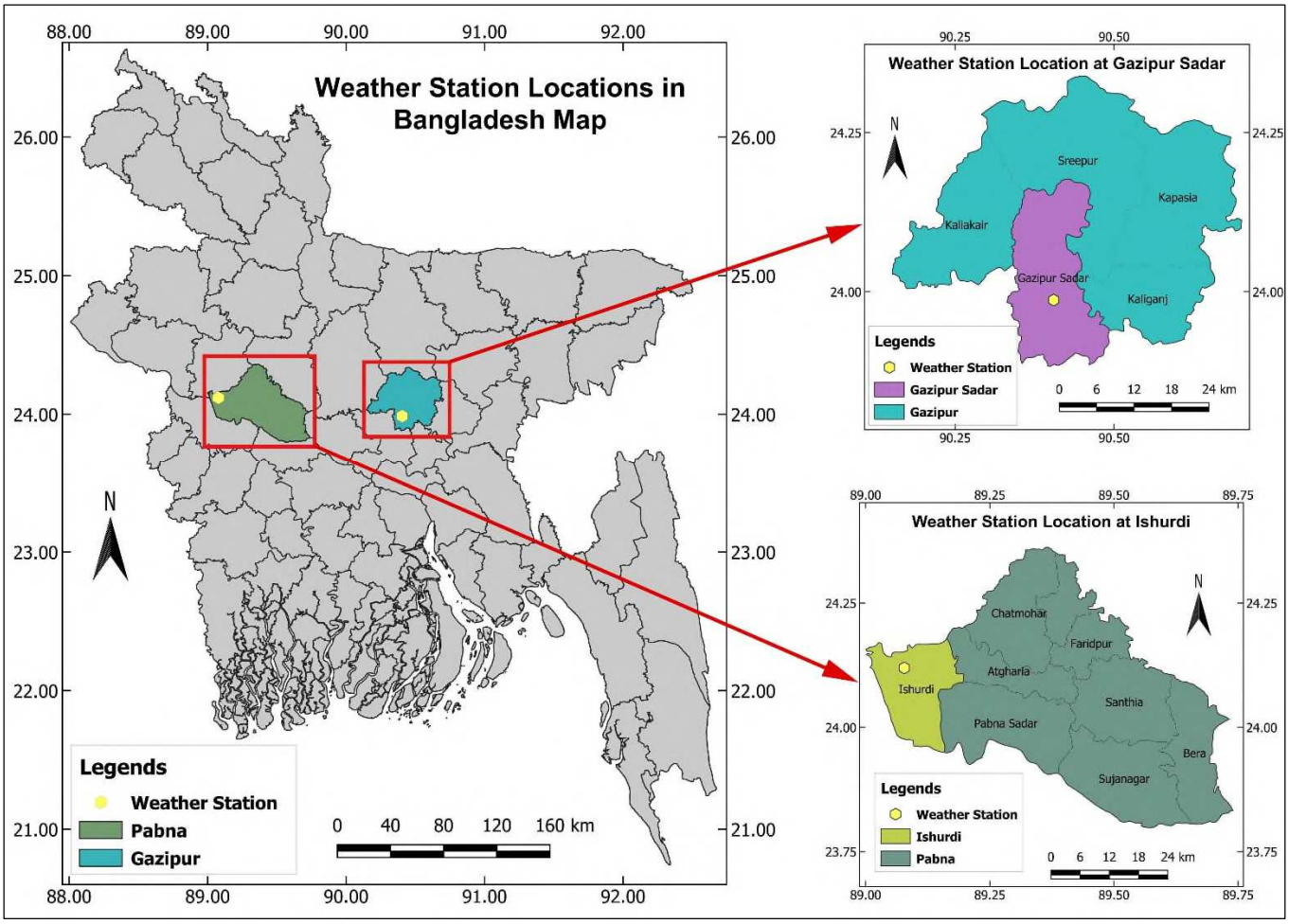

636 **Fig. 1** Locations of the weather stations within the study areas

637

638

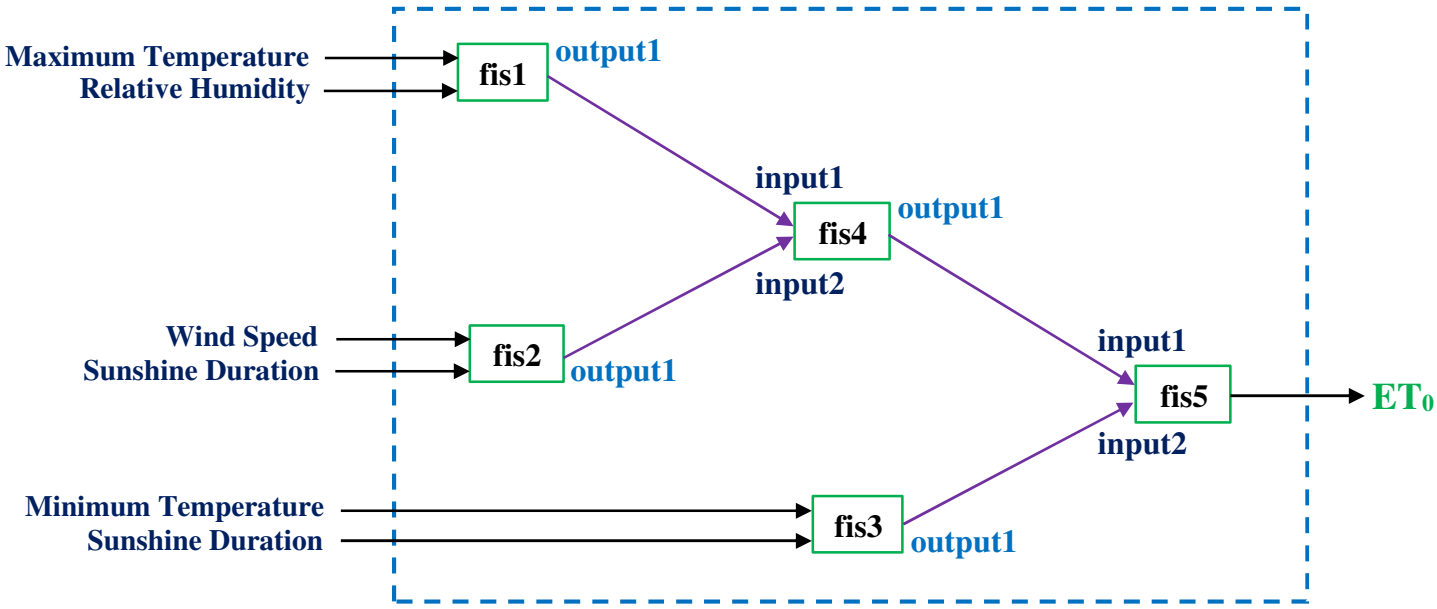

Fig. 2 FIS tree structure with multiple FIS objects

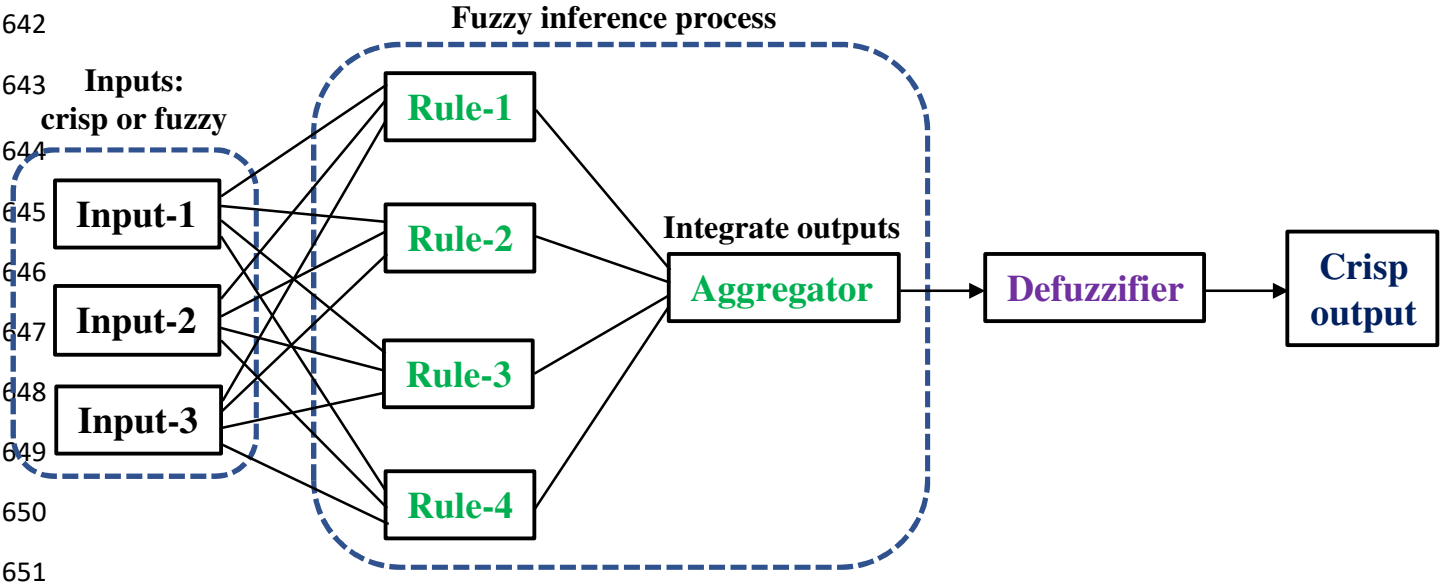

Fig. 3 Basic structure of an FIS object

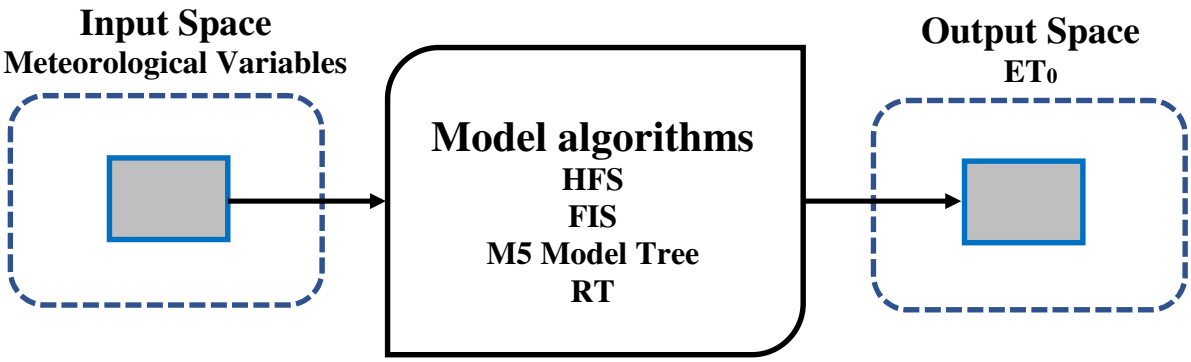

Fig. 4 Input-output mapping of prediction models for a typical ET_0 modelling approach

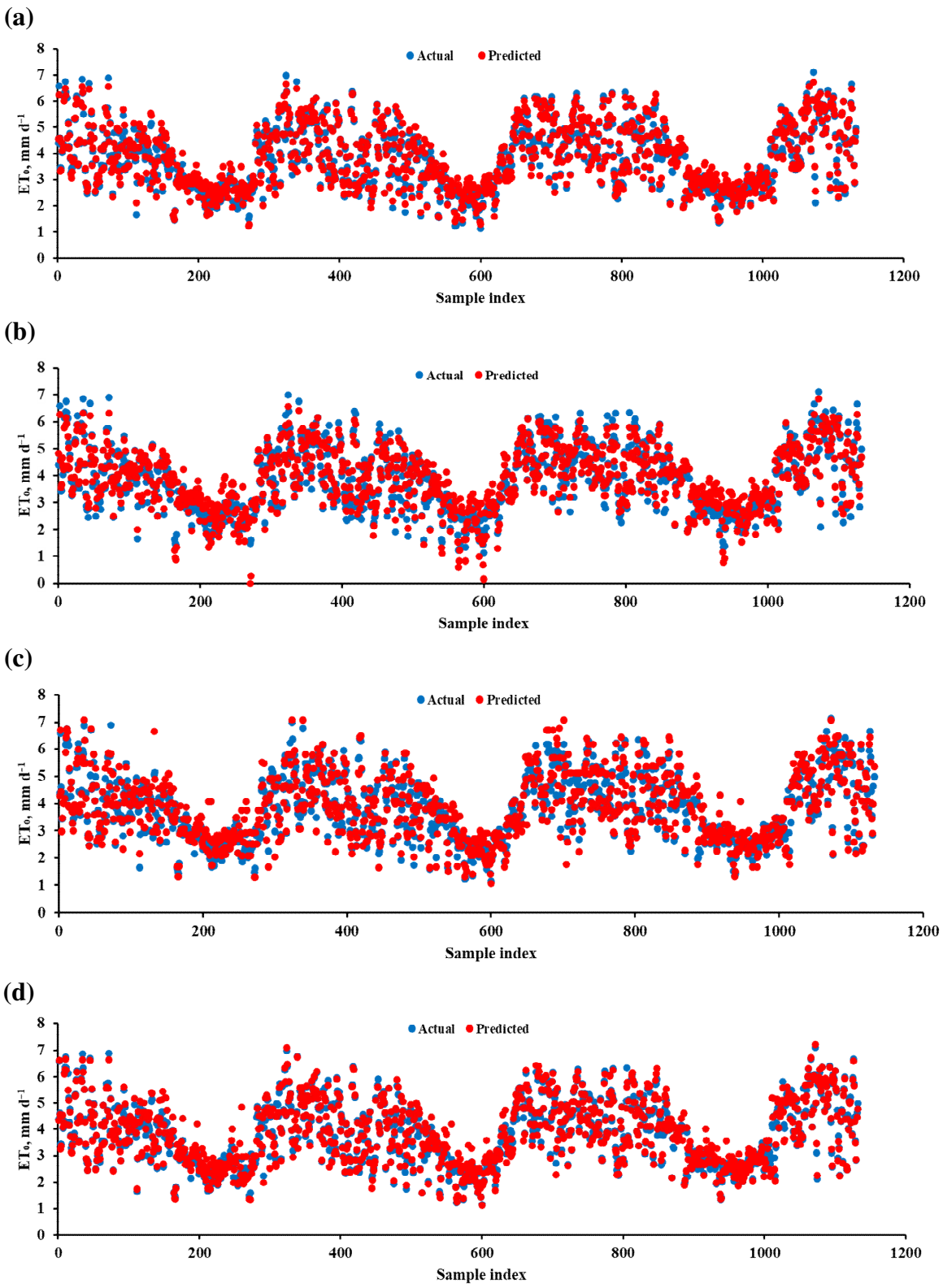

679 **Fig. 5** Scatter plots of FAO 56 PM estimated and model predicted ET_0: (a) HFS; (b) FIS; (c) RT;
680 and (d) M5 Model Tree

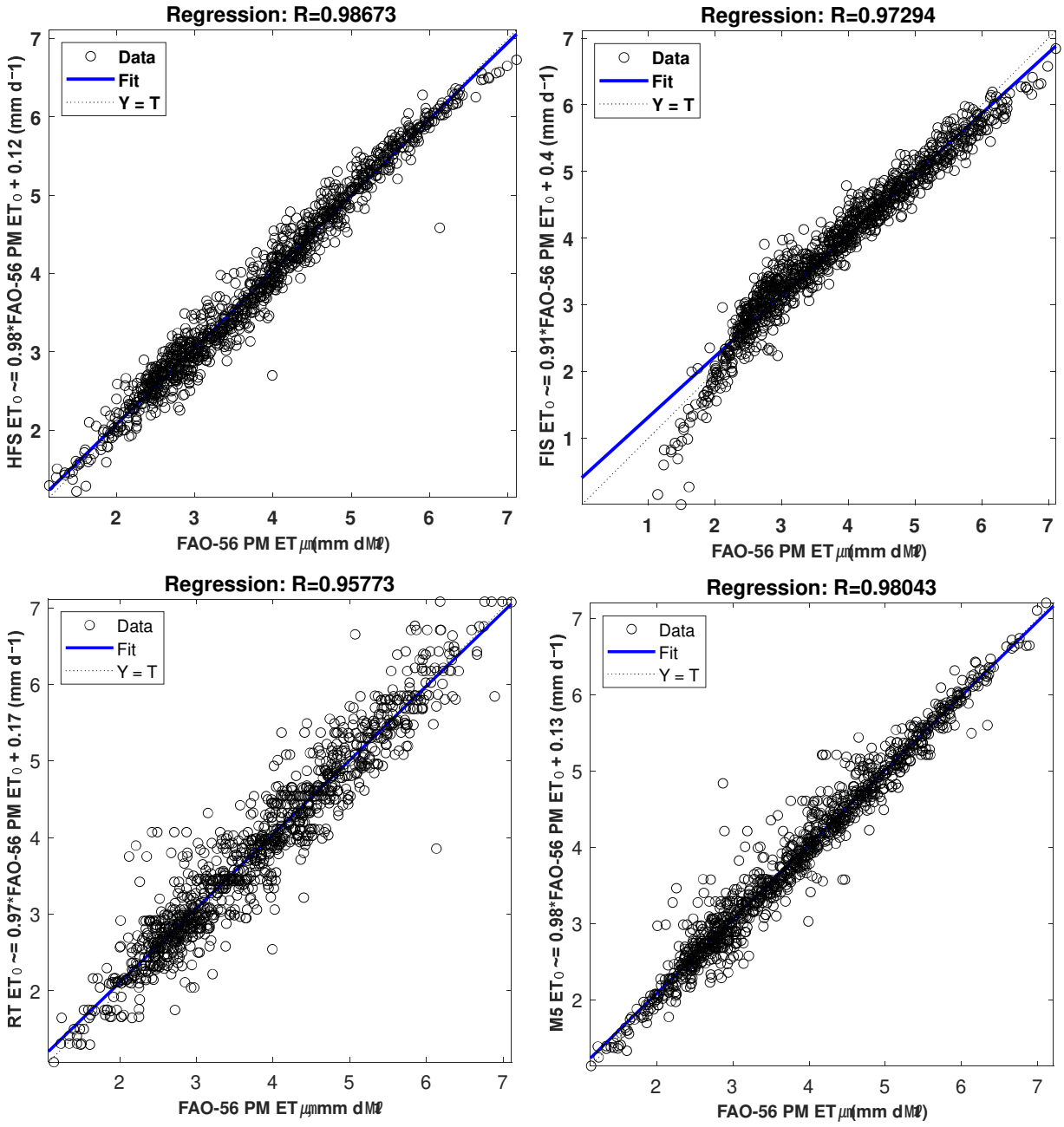

681 **Fig. 6** Regression plots of the estimated (by FAO 56 PM) and predicted (by HFS, FIS, M5
682 Model Tree, and RT) ET_0 during the test period

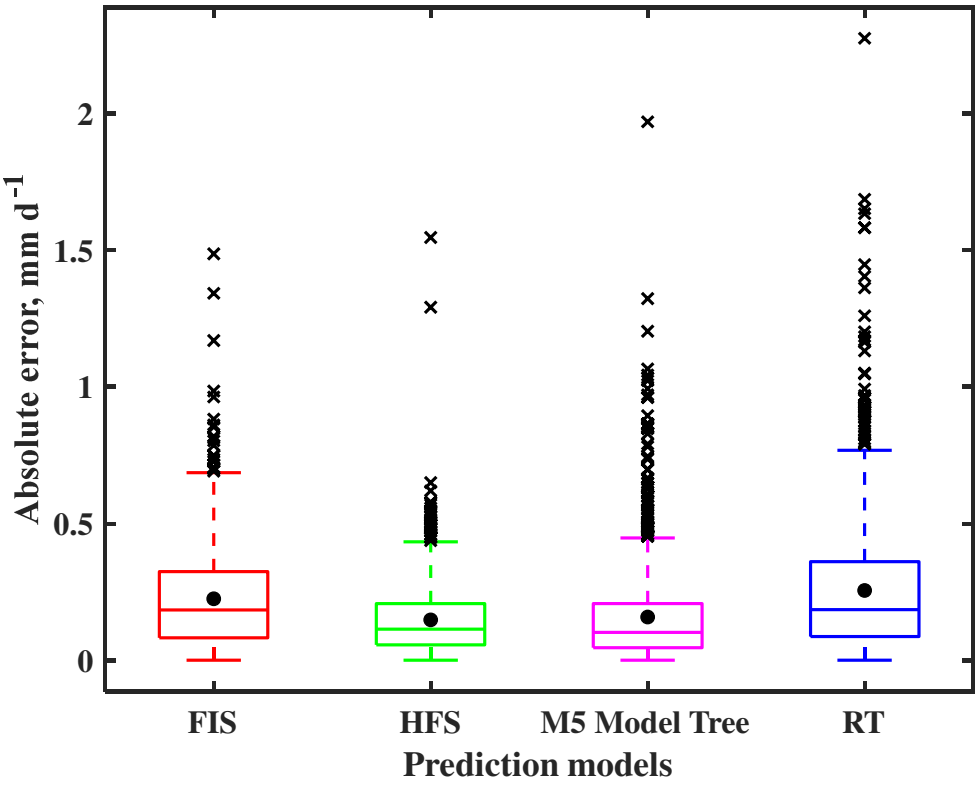

683

684 **Fig. 7** Box plots of absolute errors between the FAO 56 PM estimated and model predicted daily
685 ET_0 values. The black circles represent the mean values of absolute errors. Horizontal lines
686 inside the boxes represent the median values of absolute errors. The × symbol denotes
687 outliers

688

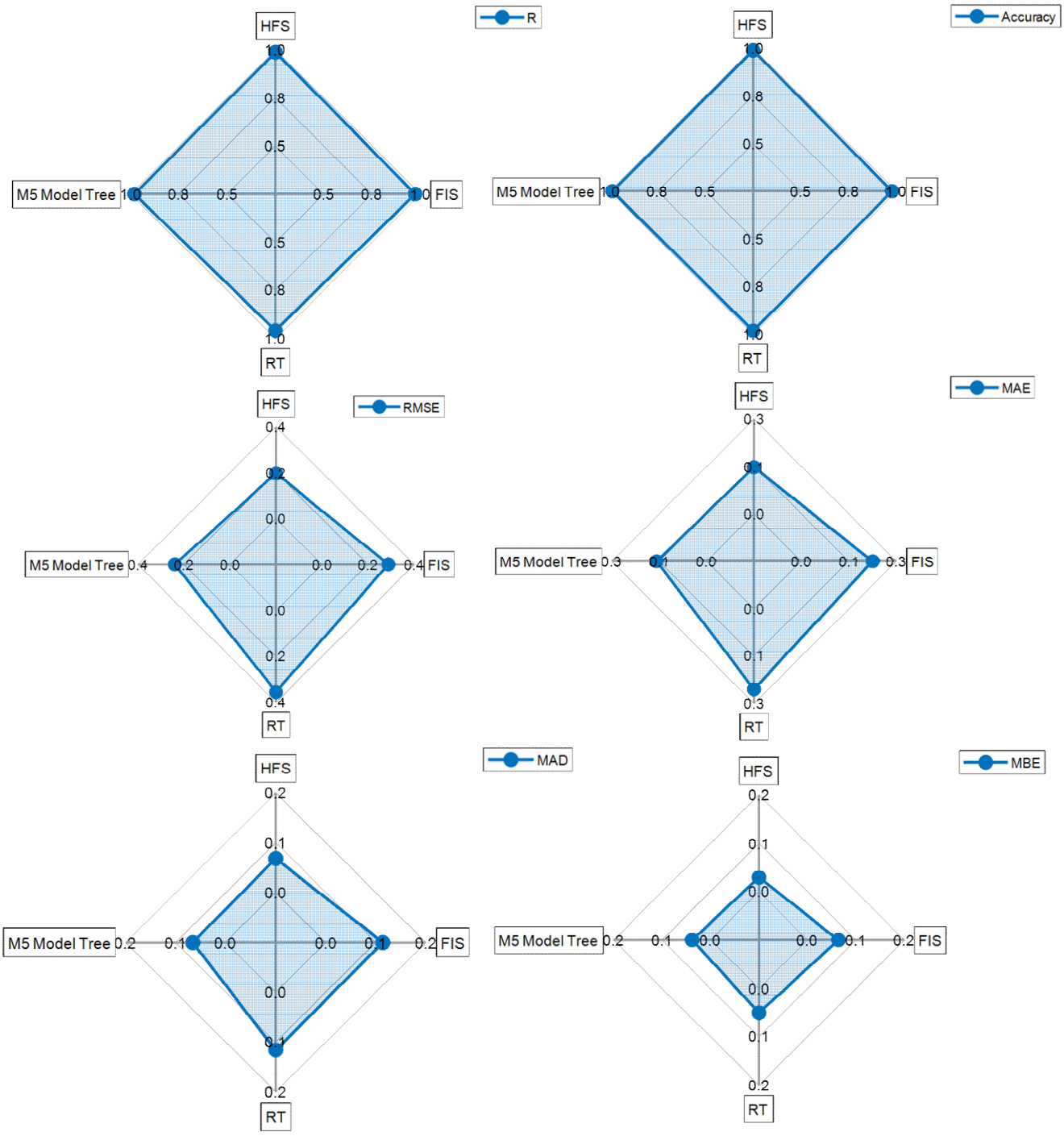

689 **Fig. 8** Spider plots of performance evaluation indices

690

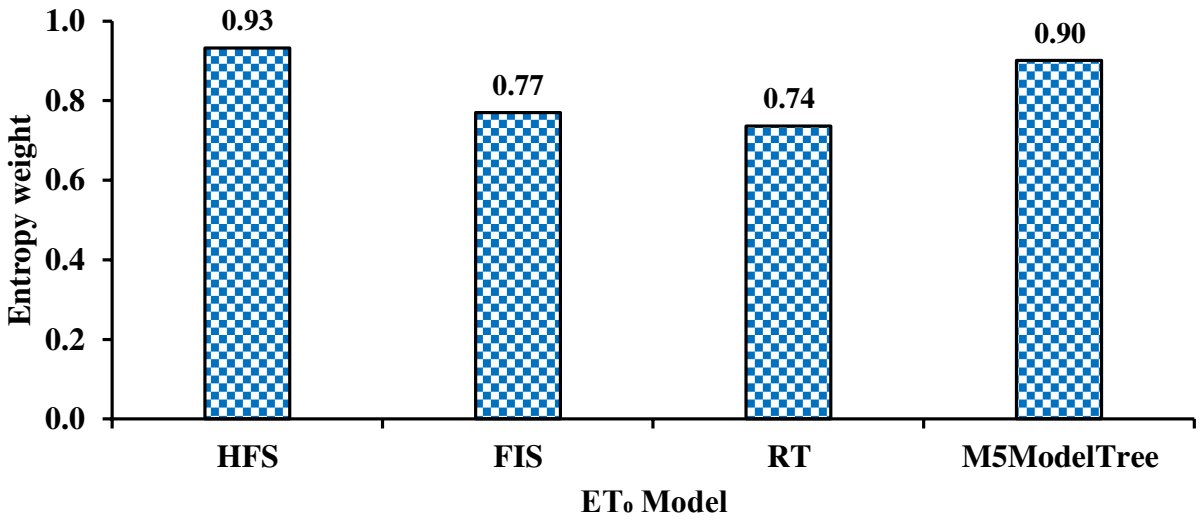

691 **Fig. 9** Ranking of models based on Entropy weight

692